1521-009X/44/8/1296–1303$25.00
Drug Metabolism and Disposition
http://dx.doi.org/10.1124/dmd.115.068338
Drug Metab Dispos 44:1296–1303, August 2016

Special Section on Emerging Novel Enzyme Pathways in Drug Metabolism

Evaluating the Disposition of a Mixed Aldehyde Oxidase/Cytochrome P450 Substrate in Rats with Attenuated P450 Activity[S]

Rachel D. Crouch, Ryan D. Morrison, Frank W. Byers, Craig W. Lindsley, Kyle A. Emmitte,[1] and J. Scott Daniels[2]

Vanderbilt Center for Neuroscience Drug Discovery (R.D.C., R.D.M., F.W.B., C.W.L., K.A.E., J.S.D.), Departments of Pharmacology (R.D.C., C.W.L, K.A.E., J.S.D.) and Chemistry (C.W.L, K.A.E.), Vanderbilt University School of Medicine, Nashville, Tennessee

Received November 11, 2015; accepted February 26, 2016

ABSTRACT

Marketed drugs cleared by aldehyde oxidase (AO) are few, with no known clinically relevant pharmacokinetic drug interactions associated with AO inhibition, whereas cytochrome P450 (P450) inhibition or induction mediates a number of clinical drug interactions. Little attention has been given to the consequences of coadministering a P450 inhibitor with a compound metabolized by both AO and P450. Upon discovering that VU0409106 (1) was metabolized by AO (to M1) and P450 enzymes (to M4–M6), we sought to evaluate the in vivo disposition of 1 and its metabolites in rats with attenuated P450 activity. Male rats were orally pretreated with the *pan*-P450 inactivator, 1-aminobenzotriazole (ABT), before an i.p. dose of 1. Interestingly, the plasma area under the curve (AUC) of M1 was increased 15-fold in ABT-treated rats, indicating a metabolic shunt toward AO resulted from the drug interaction condition. The AUC of 1 also increased 7.8-fold. Accordingly, plasma clearance of 1 decreased from 53.5 to 15.3 ml/min per kilogram in ABT-pretreated rats receiving an i.v. dose of 1. Consistent with these data, M1 formation in hepatic S9 increased with NADPH-exclusion to eliminate P450 activity (50% over reactions containing NADPH). These studies reflect possible consequences of a drug interaction between P450 inhibitors and compounds cleared by both AO and P450 enzymes. Notably, increased exposure to an AO metabolite may hold clinical relevance for active metabolites or those mediating toxicity at elevated concentrations. The recent rise in clinical drug candidates metabolized by AO underscores the importance of these findings and the need for clinical studies to fully understand these risks.

Introduction

The 2012 US Food and Drug Administration (FDA) draft guidance on defining the drug interaction potential of new chemical entities (NCEs) in drug discovery and development (http://www.fda.gov/downloads/Drugs/GuidanceComplianceRegulatoryInformation/Guidances/ucm292362.pdf) focuses primarily on human in vitro and nonclinical in vivo approaches to model clinical drug-drug interactions (DDIs) involving cytochrome P450s (P450s) and drug efflux proteins (Prueksaritanont et al., 2006; Di et al., 2013; Prueksaritanont et al., 2013); however, sparse attention has been paid to the potential for drug interactions involving compounds metabolized by enzymes falling outside these two classes of drug disposition proteins. One such enzyme receiving recent attention is the molybdenum-containing flavoprotein, aldehyde oxidase (AO). In particular, significant strides have been made toward understanding the structure-activity-relationships of AO binding and metabolism (Beedham et al., 1995; Dalvie et al., 2012; Coelho et al., 2015), species differences (Beedham et al., 1987; Garattini and Terao, 2012; Dalvie et al., 2013), human AO variability (Hartmann et al., 2012; Hutzler et al., 2014), and inhibition of AO in vitro (Obach et al., 2004; Barr and Jones, 2011), whereas studies defining the importance of this enzyme in an in vivo drug interaction scenario are lacking, perhaps owing to a deficiency of well-established specific AO inhibitors considered suitable for in vivo pharmacokinetic (PK) studies.

To date, limited PK drug interactions involving the few marketed (known) AO substrates have been recognized, despite identification of several clinical drugs demonstrating AO inhibitory activity in vitro (Obach et al., 2004). Rather, the few reported clinical interactions for

This work was supported by the Pharmaceutical Research and Manufacturers of America Foundation (PhRMA Foundation Pre-Doctoral Fellowship); the National Institutes of Health [Grant T32GM07628]; the National Institute on Drug Abuse [R01DA23947]; and the Lipscomb University College of Pharmacy-Vanderbilt University Department of Pharmacology Joint PharmD-PhD Program.

[1]Current affiliation: University of North Texas System College of Pharmacy, Fort Worth, Texas.

[2]Current affiliation: Sano Informed Prescribing, Inc., Franklin, Tennessee.

dx.doi.org/10.1124/dmd.115.068338.

[S]This article has supplemental material available at dmd.aspetjournals.org.

ABBREVIATIONS: ABT, 1-aminobenzotriazole; AO, aldehyde oxidase; AUC, area under the time-concentration curve; C_{max}, maximal plasma concentration; CL_{int}, intrinsic clearance; CL_p, plasma clearance; DDI, drug-drug interaction; FDA, Food and Drug Administration; HPLC, high-performance liquid chromatography; K_m, Michaelis constant, LC/MS, liquid chromatography mass spectrometry; LC-MS/MS, liquid chromatography-tandem mass spectrometry; P450, cytochrome P450; PK, pharmacokinetics; rcf, relative centrifugal force; SD, Sprague Dawley; $t½$, half-life; T_{max}, time to reach maximal plasma concentration; V_{max}, maximal reaction velocity; XO, xanthine oxidase.

AO-cleared drugs involve inhibition or induction of a secondary non-AO metabolism pathway (Ramanathan et al., 2016). For example, FDA labeling for zaleplon recommends a dose adjustment when coadministered with cimetidine, which inhibits not only AO, but also P450 3A4, the secondary route of zaleplon metabolism (http://www.accessdata.fda.gov/drugsatfda_docs/label/2007/020859s011lbl.pdf). Additionally, changes in exposure to the chemotherapeutic idealisib were noted with coadministration of the P450 3A inhibitor ketoconazole or the inducer rifampin (Ramanathan et al., 2016). A noteworthy report recently indicated an important role for AO in a drug interaction between BILR 355 and the P450 3A inhibitor ritonavir, where coadministration resulted in a metabolic "switch" from P450 3A metabolism of BILR 355 to gut bacterial and subsequent AO metabolism (Li et al., 2012a,b). Furthermore, Li's studies monitoring formation of this AO metabolite in human S9 in the presence and absence of NADPH were consistent with a metabolic shunt toward AO when the P450 pathway was inactive. This report brought attention to the possibility of a drug interaction leading to a metabolic switch and the potential for AO to contribute to such an event.

We previously reported the disposition of a novel $mGlu_5$-negative allosteric modulator, VU0409106 (**1**), which was discovered to be predominantly metabolized by AO (Scheme 1), to the primary metabolite, **M1** (Morrison et al., 2012). Notably, we demonstrated that the in vitro scaled hepatic clearance (CL_{HEP}) of **1** was in general agreement with the in vivo plasma clearance (CL_p) observed in Sprague-Dawley (SD) rats and cynomolgus monkey. Our continued interest in **1** has been driven largely by the observation that P450 pathways also contribute to its biotransformation, resulting in formation of metabolites **M4**, **M5,** and **M6**. Whereas Li's report demonstrates a drug interaction that elicits a metabolic switch in a unique scenario requiring an intermediate gut bacterial metabolism step, we hypothesized that hepatic P450 inhibition may result in an elevated exposure to the AO metabolite of a drug cleared via both AO and P450 enzymes. Because AO and P450 commonly generate different metabolites owing to opposing substrate specificities (AO prefers to oxidize electron-deficient carbons, whereas P450 prefers electron-rich sites), this creates a potential scenario for increased exposure to one metabolite when the other metabolic pathway is inhibited. The observation that **1** was metabolized exclusively by AO to **M1** and to **M4**–**M6** by P450 enzymes presented an opportunity to investigate the disposition of a mixed AO:P450 substrate and the corresponding AO and P450 metabolites in a drug interaction scenario of P450 inhibition. Given the similarities in rodent metabolism and clearance of **1** to that observed in human S9 and hepatocytes (Morrison et al., 2012), we designed this drug interaction scenario in vivo in SD rats, a conventional species historically used in nonclinical PK investigations (Di et al., 2013), via coadministration of **1** and the *pan*-P450 inactivator 1-aminobenzotriazole (ABT). Observations from the present in vitro and in vivo investigations indicate evidence of metabolic shunting toward AO metabolism in the disposition of **1** in rat when P450 activity is attenuated, resulting in elevated exposure to the AO metabolite **M1**.

Materials and Methods

Materials

VU0409106 (**1**) was prepared and characterized by the Department of Medicinal Chemistry within the Vanderbilt Center for Neuroscience Drug Discovery. Potassium phosphate, ammonium formate, formic acid, magnesium chloride, 1-aminobenzotriazole (ABT), hydralazine, and allopurinol were purchased from Sigma-Aldrich (St. Louis, MO). NADPH tetrasodium salt was purchased from VWR (Radnor, PA). Pooled human (150-donor, mixed gender) or male SD rat hepatic microsomes and S9 were obtained from BD Biosciences (San Diego, CA). All solvents or reagents were of the highest purity commercially available.

Biotransformation of 1 in Multispecies Hepatic Microsomes and S9 Fractions

Hepatic Micromsomal Metabolism of 1. The in vitro metabolism of **1** was investigated in rat and human hepatic microsomal fractions. A potassium phosphate-buffered reaction (100 mM, pH 7.4) of **1** (10 μM), hepatic microsomes (1 mg/ml), $MgCl_2$ (3 mM), and NADPH (2 mM) was incubated at 37°C in borosilicate glass test tubes under ambient oxygenation for 60 minutes. The total incubation volume was 0.5 ml. Reactions were initiated by the addition of **1**, terminated with the addition of 2 volumes of acetonitrile, and subsequently centrifuged at 3500 relative centrifugal force (rcf) for 10 minutes. The resulting supernatant was dried under a stream of nitrogen and reconstituted in 85:15 (v/v) ammonium formate (10 mM, pH 4.1):acetonitrile in preparation for LC/MS analysis.

M1 Formation in Multispecies Hepatic S9 Fractions. Similarly, the metabolism of **1** and subsequent formation of **M1** in rat and human hepatic S9 fractions (2.5 mg/ml; ±1 mM NADPH) was investigated. Total incubation volume was 200 μl. Reactions were initiated with the addition of **1** (1 μM), and at designated times (t = 0, 7, 15, 30, 45, and 60 minutes), aliquots were removed and precipitated with ice-cold acetonitrile containing an internal standard (carbamazepine, 50 ng/ml). The mixture was centrifuged at 3500 rcf for 5 minutes, and resulting supernatants were diluted with water in preparation for liquid chromatography-tandem mass spectrometry (LC-MS/MS) analysis.

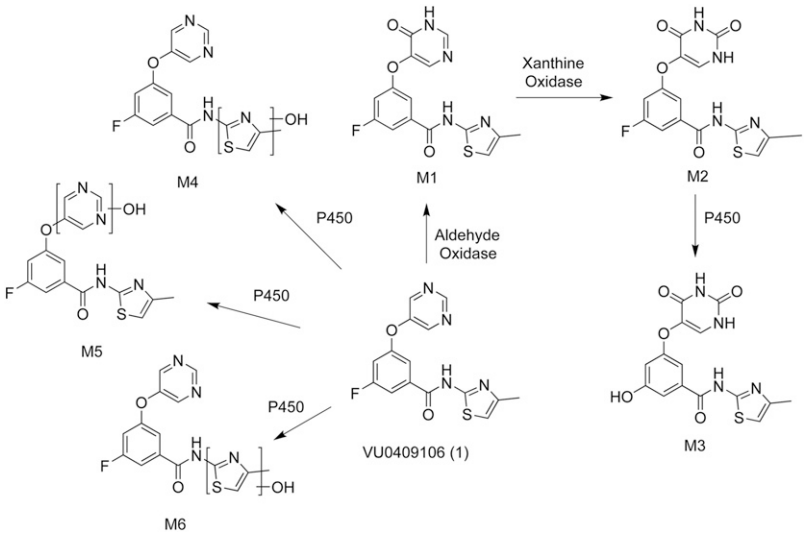

Scheme 1. Metabolism of VU0409106 (**1**) in vitro in SD rats and human.

Intrinsic Clearance in Multispecies Hepatic S9 Fractions. To explore potential kinetic mechanisms responsible for our observations of **M1** formation in S9, we measured the intrinsic clearance (CL_{int}) of **1** in rat and human S9 fractions at three different concentrations of **1** using NADPH and hydralazine to isolated the NADPH-dependent (P450), NADPH-independent (AO), and total (P450 + AO) hepatic S9 CL_{int} for each species. For measurement of total NADPH-independent and NADPH-dependent S9 CL_{int}, compound **1** (0.1 μM, 1 μM, or 10 μM) was incubated as described in rat or human S9 fractions in the presence or absence of NADPH or in the presence of NADPH after preincubation with the AO-specific inhibitor hydralazine (50 μM), respectively. Rat and human S9 CL_{int} (ml/min per kilogram) was estimated using the substrate depletion method and eq. 1:

$$CL_{int} = \frac{ln2}{t_{1/2\ (min)}} \times \frac{mL}{2.5\ mg\ protein_{S9}} \times \frac{120\ mg\ protein_{S9}}{g\ liver\ weight} \times \frac{(A)g\ liver\ weight}{kg\ body\ weight} \quad (1)$$

where $t_{1/2}$ is the substrate depletion half-life and A = 20 (human) or 45 (rat).

In Vivo Metabolism of 1 in SD Rats

All animal studies were approved by the Vanderbilt University Medical Center Institutional Animal Care and Use Committee. To evaluate the pharmacokinetics of **1,** 8- to 12-week-old male SD rats (n = 2) weighing between 250 and 325 g were purchased from Harlan (Indianapolis, IN); catheters were surgically implanted in the carotid artery and jugular vein. The cannulated animals were acclimated to their surroundings for approximately 1 week before dosing and provided food and water ad libitum. Similarly, in-life studies in SD rats receiving an i.p. dose of 3 mg/kg (n = 3 for control group, n = 4 for ABT group) or 10 mg/kg (n = 2) of **1** were conducted at Frontage Laboratories (Exton, PA).

Administration of 1 to SD Rats. Inhibitors of P450 (ABT) and/or xanthine oxidase (allopurinol) were administered orally to male SD rats at 50 mg/kg at a dose volume of 5 ml/kg (ABT, 1% methylcellulose) or 2.5 ml/kg (allopurinol, 1% methylcellulose). Two hours after inhibitor administration (approximate T_{max} of both ABT and allopurinol), a dose of **1** (10% ethanol/70% PEG400/20% saline) was administered at 3 or 10 mg/kg i.p. or i.v. at 1 mg/kg. Blood (200 μl) was collected via the carotid artery at 0.0833, 0.25, 0.5, 1, 2, 4, 6, 8, 10, 12, and 24 hours postadministration of compound **1**. Samples were collected in chilled, EDTA-fortified tubes and centrifuged for 5 minutes (1700 rcf, 4°C), and the resulting plasma was stored at −80°C until LC-MS/MS analysis. The resulting plasma samples were protein precipitated with ice-cold acetonitrile containing internal standard (carbamazepine, 50 ng/ml), centrifuged (3500 rcf for 5 minutes), and the resulting supernatants diluted with water in preparation for LC-MS/MS analysis.

LC-UV-TMS/MS Analysis of 1 and Metabolites

Exposure Analysis of Plasma and S9 Fractions. The quantitation of **1** and its metabolites (**M1**, **M2**, **M4–M6**) from plasma and S9 fraction incubations was conducted via electrospray ionization on an AB Sciex API-5500 QTrap (Applied Biosystems, Foster City, CA) instrument that was coupled with LC-20AD pumps (Shimadzu, Columbia, MD) or an AB Sciex API-4000 triple quadrupole instrument coupled with Shimadzu LC-10AD pumps and a CTC PAL autosampler (Leap Technologies, Carrboro, NC). Analytes were separated by gradient elution using a Fortis C18 column (3 × 50 mm, 3 μm; Fortis Technologies Ltd., Cheshire, UK) warmed to 40°C. Mobile phase A was 0.1% formic acid in water (pH unadjusted); mobile phase B was 0.1% formic acid in acetonitrile. The gradient started at 30% B after a 0.2-minute hold and was linearly increased to 90% B over 1.5 minutes, held at 90% B for 0.5 minute, and returned to 30% B in 0.1 minute followed by a re-equilibration (0.4 minute) with a total run time of 2.7 minutes or alternatively started at 30% B after a 0.2 minute hold and linearly increased to 90% B over 0.8 minute, held at 90% B for 0.5 minute, and returned to 30% B in 0.1 minute followed by a re-equilibration (0.9 minute), with a total run time of 2.5 minutes. High-performance liquid chromatography (HPLC) flow rate was 0.5 ml/min. The source temperature was set at 500°C, and mass spectral analyses were performed using multiple-reaction monitoring, with transitions and voltages specific for **1** or its metabolites using a Turbo Ion Spray source in positive ionization mode (5.0 kV spray voltage). Data were analyzed using Sciex Analyst 1.5.1 software. Concentrations of **1** were determined using a matrix-matched 9-point standard curve (lower limit of quantitation = 0.5 ng/ml). As no authentic standard was available to determine metabolite concentrations, a semiquantitative analysis was expressed as the analyte peak:internal standard ratio (internal standard, carbamazepine) (Morrison et al., 2012).

TABLE 1

Liquid chromatography-mass spectrometry detection of metabolites in vivo (Sprague-Dawley rat) or in vitro in Sprague-Dawley rat and human microsomes

Matrix	Metabolites Detected					
	M1	M2	M3	M4	M5	M6
Rat plasma	√	√	√	√	√	√
Rat microsomes	√[a]				√	√
Human microsomes	√[a]				√	√

[a]Cytosolic AO contamination of microsomes produced low levels of M1.

Metabolite Detection. LC/UV/MS analysis of metabolites generated in vitro was performed with an Agilent 1100 HPLC system coupled to a Supelco Discovery C18 column (5 μm, 2.1 × 150 mm; Sigma-Aldrich). Solvent A was 10 mM (pH 4.1) ammonium formate, and solvent B was acetonitrile. The initial mobile phase was 85:15 A-B (v/v), and by linear gradient was transitioned to 20:80 A-B over 20 minutes for a total run time of 30 minutes. The flow rate was 0.400 ml/min. The HPLC eluent was first introduced into an Agilent 1100 diode array detector

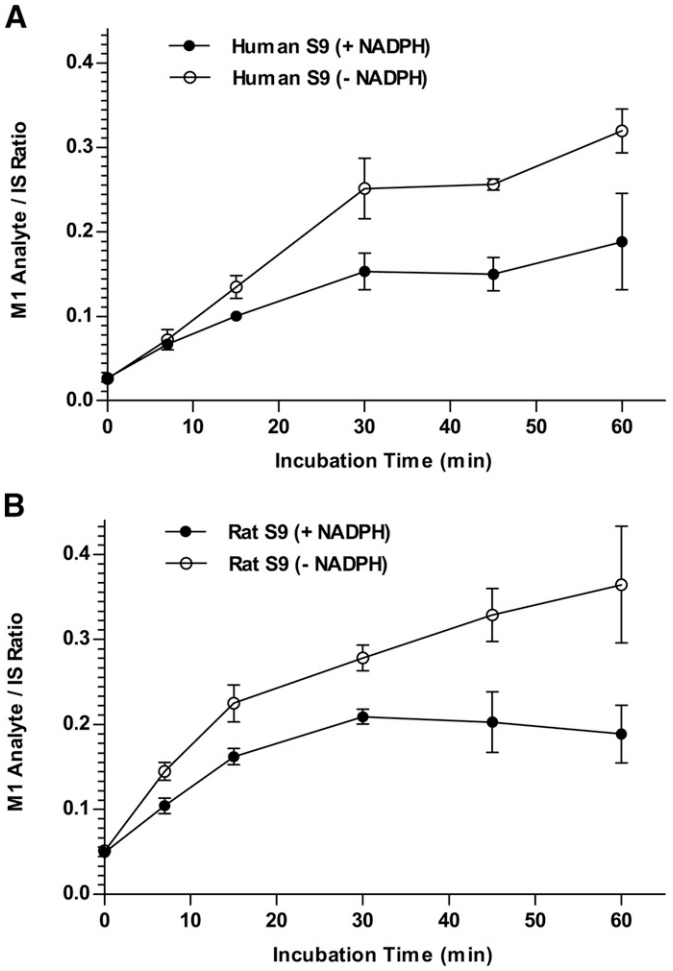

Fig. 1. Formation of M1 in incubations of VU0409106 (**1**) with human hepatic S9 (A) or SD rat hepatic S9 (B) in the presence (closed circles) or absence (open circles) of NADPH. Data points are expressed as the peak area ratio of analyte/internal standard and represent the mean of a triplicate determination (± S.D.).

TABLE 2

Exposure of M1 formed from human or rat hepatic S9 incubations of **1** in the presence or absence of NADPH

In Vitro Incubation	+ NADPH	- NADPH
Human S9	7.7 ± 0.66	12.2 ± 0.68
Rat S9	10.4 ± 0.90	15.7 ± 0.68

AUC expressed as the peak area ratio analyte/IS*min and represent means of triplicate determinations (± S.D.).

(254 nM) followed by electrospray ionization-assisted introduction into a LCQ Deca XP^{PLUS} ion trap mass spectrometer (Thermoelectron Corp., San Jose, CA) operated in positive ionization mode. Ionization was assisted with sheath and auxiliary gas (ultrapure nitrogen) set at 60 and 40 psi, respectively. The electrospray voltage was set at 5 kV with the heated ion transfer capillary set at 300°C and 30 V. Data were analyzed using Thermo XCalibur 2.0 software.

Data Analysis

GraphPad Prism version 5.04 (GraphPad Software, San Diego, CA) was used in the semiquantitation of **M1** resulting from the S9 fraction metabolism of **1**, as well as in the generation of time-concentration profiles of **1** and its metabolites in rat plasma. Subsequent area under the curve (AUC) values of M1 from S9 experiments were also generated in GraphPad Prism (trapezoid rule). PK parameters of **1** were obtained using WinNonLin (noncompartmental analysis; Phoenix version 6.2; Pharsight, Mountain View, CA).

Statistical Analysis

GraphPad Prism version 5.04 (GraphPad Software) was used in the statistical analyses of in vivo PK parameters; a two-tailed unpaired *t* test was used, with a significance level of $P < 0.05$.

Results

A Mixed AO:P450 Metabolism Phenotype of 1 In Vitro

Rat and Human Hepatic Microsomes. We previously reported that the primary biotransformation pathway of compound **1** was catalyzed by AO to the principal metabolite **M1**, plus other metabolites (e.g., **M4/M5**) mediated by P450 and detected in nonclinical species and human hepatic S9 fractions (Scheme 1), as well as in vivo in SD rats receiving i.p. administrations of **1** (Morrison et al., 2012). Furthermore, we demonstrated the in vitro-in vivo correlation of the predicted hepatic and plasma clearance of **1** in rats and nonhuman primates, a finding that established the relevancy of a principal AO mechanism of clearance in vivo, with a secondary contribution from P450 in the disposition of **1**. Presently, we used LC/UV/MS and hepatic microsomes to define the role of P450 in the metabolism of **1** in rat and human and to monitor P450 metabolites in the investigation of a metabolic shunt involving AO. Data from hepatic microsomal incubations of **1** indicated the NADPH-dependent formation of the hydroxylated metabolites **M5** and **M6**. The identification and proposed structure elucidation of **M6** were facilitated by LC-MS/MS analysis, with a subsequent deuterium-exchange LC/MS experiment indicating the oxidation of a carbon atom of the thiazole moiety (Table 1; Supplemental Fig. 1, LC/MS data of **M6**); the data collected from these experiments were consistent with a P450-mediated oxidation of **1** versus the potential involvement of a flavin monooxygenase. The retention time and respective MS/MS fragmentation data for **M5** were consistent with our previous report detailing the biotransformation of **1** (Morrison et al., 2012). Whereas the thiazole-hydroxylated metabolite, **M4**, has been observed in vivo in rat plasma, as well as in rat and human hepatocytes (attenuated with ABT pretreatment) (Morrison et al., 2012), it was below our detection limits in rat or human hepatic microsomes in the present study. The appearance of **M1** in rat and human microsomal incubations was NADPH-independent and indicative of trace contamination of the microsomal fraction with cytosol (containing AO); this finding of background AO activity in contaminated hepatic microsomes is not uncommon (Diamond et al., 2010) and was confirmed by the suppression of **M1** formation with the AO-specific inhibitor hydralazine (data not shown).

Intrinsic Clearance of 1 and Relative Formation Rates of M1 in Rat and Human S9 Fractions Implicate a Metabolic Shunting Mechanism Mediated by AO. When compound **1** was incubated under kinetically controlled conditions (1 μM, 60 minutes of incubation) in both rat and human hepatic S9 fractions (±NADPH), the observed magnitude of **M1** formation in S9 incubations, absent the P450 reducing cofactor NADPH, was greater than that observed when incubations were fortified with NADPH (Fig. 1). An approximate 50% increase in the AUC of **M1** was observed in S9 incubations absent NADPH relative to those incubations containing NADPH from both human and rat experiments (Table 2). We previously demonstrated that subsequent metabolism of **M1** to **M2** is catalyzed by xanthine oxidase (XO; Scheme 1)(Morrison et al., 2012), an enzyme that does not require the reducing cofactor NADPH for catalytic activity, thus excluding P450-mediated conversion of **M1** to **M2** as the mechanism responsible for this observation. The observed increase in **M1** in S9 incubations absent NADPH may likely be due to an increase in substrate exposure to AO in the absence of NADPH-dependent P450 metabolism. To explore this possibility, we measured the CL_{int} of **1** in rat and human S9 fractions in the presence and absence of NADPH and in the presence of NADPH and the AO inhibitor, hydralazine, to estimate the CL_{int} mediated by both AO and P450, AO only, and P450 only, respectively (Table 3) and over a concentration range of **1** (0.1 μM, 1 μM, and 10 μM). Whereas NADPH-dependent CL_{int} in both species decreased with increasing concentration of **1**, NADPH-independent CL_{int} remained constant in rat incubations, with some decrease in human S9 incubations. The decrease in NADPH-dependent CL_{int} at higher concentrations was also reflected by a decrease in the total CL_{int} observed when both P450 and AO are active. These data indicate the likelihood that the overall K_m for the P450 pathways is lower than

TABLE 3

Total, NADPH-dependent, and NADPH-independent rat and human hepatic S9 intrinsic clearance of **1** at concentrations of 0.1 μM, 1 μM, and 10 μM

Data represent means of triplicate determinations (± S.D.).

Concentration	Rat			Human		
	+NADPH + hydralazine CL_{int}	+NADPH CL_{int}	-NADPH CL_{int}	+NADPH +hydralazine CL_{int}	+NADPH CL_{int}	-NADPH CL_{int}
0.1 μM	41.5 ± 4.6	99.6 ± 8.3	25.3 ± 2.6	39.3 ± 1.1	48.8 ± 7.6	7.2 ± 1.1
1 μM	22.4 ± 1.7	52.1 ± 6.1	24.5 ± 2.6	7.7 ± 1.4	15.3 ± 2.0	6.4 ± 1.2
10 μM	<4.9	24.7 ± 2.0	24.4 ± 4.0	<2.2	5.9 ± 0.4	4.1 ± 0.7

that for the AO pathway and are consistent with a mechanism of metabolic shunting toward AO under conditions of attenuated P450 metabolism and greater substrate availability for AO. Although the NADPH-independent CL_{int} observed in the present experiments was slightly elevated compared with previously reported (Morrison et al., 2012), this finding is not surprising given the potential in vitro variability of AO recently described across multiple individual hepatocyte donors, for example (Hutzler et al., 2014); variability in AO-mediated CL_{int} values for the same AO substrate has also been reported (Kitamura et al., 1999; Al-Salmy, 2001; Sahi et al., 2008). Taken together, the present in vitro data indicate that the SD rat represents an acceptable nonclinical model to study the in vivo disposition of **1** and its metabolites under drug-interaction duress (e.g., P450 inhibition), particularly the occurrence of metabolic shunting from P450 toward AO.

ABT Pretreatment Results in Increased Exposure to Parent 1 and the AO Metabolite M1 In Vivo in SD Rats

To evaluate the impact of P450 inhibition on the disposition of **1** and its metabolites, SD rats received an i.p. administration of **1** (3 mg/kg), with or without oral ABT (50 mg/kg) pretreatment. We then generated standard plasma time-concentration profiles (Fig. 2) using contemporary LC-MS/MS quantitation, reporting standard PK parameters [e.g., maximal plasma concentration (C_{max}), AUC_{0-inf}, CL_p, V_{ss}, $t_{1/2}$, Table 4, 5, and 6). Statistically significant changes were observed in the plasma clearance (CL_p), AUC, and maximal concentration (C_{max}) of rats pretreated with ABT versus vehicle pretreatment. In rats pretreated with ABT, a 7.8-fold increase in the plasma AUC of **1** was observed (Fig. 2A, Table 4). Likewise, the C_{max} was increased 3.1-fold. The PK of **1** was also obtained (Table 4) following a parenteral administration of **1** to rats, where an increase in AUC of **1** was again observed (3.5-fold), along with a corresponding reduction in the average CL_p from 53.5 to 15.3 ml/min/kg in rats pretreated with ABT.

We also observed an increase in the exposure to the AO metabolite **M1** in rats receiving the ABT pretreatment, with 15-fold and 7.3-fold increases in the average AUC and C_{max} values, respectively (Fig. 2B; Table 5). We submit that this finding is consistent with the contributions of a shunting mechanism toward the AO pathway when P450 activity is attenuated by ABT (as was observed in hepatic S9 incubations of **1** that were absent NADPH). We previously reported that **M1** is converted to **M2** via XO, followed by an oxidative-defluorination to **M3** (Scheme 1) (Morrison et al., 2012). Consequently, a substantial increase in **M2** was also observed in rats as a result of ABT pretreatment (11-fold and 14-fold increase in mean C_{max} and AUC, respectively) (Fig. 2D; Table 5). Although the increase in **M2** can be explained by an increase in its precursor metabolite, **M1**, we considered the possibility that accumulation of **M2** in ABT-pretreated rats occurred as a result of reduced P450-mediated conversion of **M2→M3**, with the potential to reduce the rate of **M1** conversion to **M2** (e.g., product inhibition). To investigate the contributions of secondary P450-mediated metabolism of **M2** to the observed plasma levels of **M1**, rats were orally administered either ABT (50 mg/kg), the XO inhibitor allopurinol (50 mg/kg), or a combination of the two inhibitors before the i.p. injection of compound **1** (10 mg/kg). Similar to rats receiving the 3 mg/kg dose of **1**, rats receiving the 10 mg/kg dose displayed a 14-fold increase in the AUC of **M2** when pretreated with ABT (Fig. 3A; Table 6). **M2** was below the detection limits in rats pretreated with the XO inhibitor allopurinol and was detectable only at the latter time points collected from rats pretreated with both allopurinol and ABT (data not shown). Pretreatment with allopurinol revealed a relatively small increase of 2.6-fold in the AUC of **M1** compared with a 9.1-fold increase after ABT pretreatment (Fig. 3B; Table 6). Importantly, when

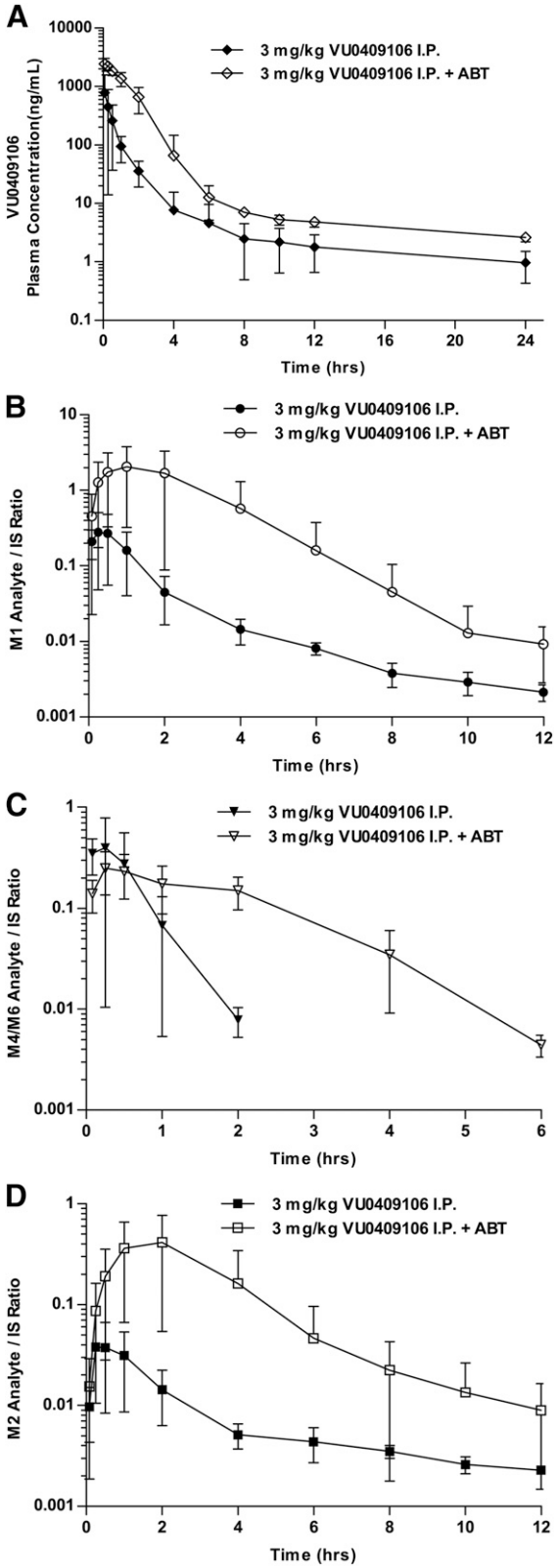

Fig. 2. Mean plasma concentration-time profiles of VU0409106 (**1**) (A), **M1** (B), **M4–M6** (C), and **M2** (D) after administration of **1** to control (closed symbol) or ABT pretreated (open symbol) SD rats. Each data point represents the mean (±S.D.; n = 2 or 3 (control), n = 3 or 4 ABT pretreated).

TABLE 4

Pharmacokinetic (PK) parameters of VU0409106 after i.v. (1 mg/kg) or i.p. (3 mg/kg) administration of **1** to control rats or rats pretreated with ABT

Data for control and ABT groups represent a mean of n = 2 (± S.E.M.). Data for control (n = 3) and ABT (n = 4) groups represent a mean (± S.D.). Statistical analysis was performed using a two-tailed unpaired t test.

Compound Dosed and Quantitated	Dose (Route)	PK Parameter	Control	ABT	Mean Fold over Control
1	1 mg/kg (i.v.)	CL (ml/min/kg)	53.5 ± 1.12	15.3 ± 1.19 **	0.29
		V_{ss} (liter/kg)	0.994 ± 0.052	0.946 ± 0.005	0.95
		$t_{1/2}$ (h)	0.215 ± 0.016	0.721 ± 0.061*	3.4
		AUC_{0-inf} (h*ng/ml)	311 ± 6.52	1099 ± 85.7 *	3.5
	3 mg/kg (i.p.)	C_{max} (ng/ml)	787 ± 782	2453 ± 589 *	3.1
		AUC_{0-inf} (h*ng/ml)	482 ± 247	3742 ± 970 **	7.8

AUC, area under the plasma concentration-time curve; CL, plasma clearance; C_{max}, maximal plasma concentration; $t_{1/2}$, half-life ($t_{1/2}$ = MRT* *ln*2); *V*ss , volume of distribution at steady-state.
*$P < 0.05$, **$P < 0.01$.

rats were pretreated with both allopurinol and ABT, the AUC of **M1** increased 15-fold (Fig. 3B; Table 6; see Supplemental Fig. 2 for ABT and allopurinol exposure). These data indicate that the accumulation of **M1** from inhibition of the **M2→M3** pathway is likely a minimal contributing factor toward the increase in **M1** exposure in rats experiencing the ABT-induced DDI duress.

The P450-mediated metabolites **M4** and **M6** were monitored to ascertain the impact of ABT pretreatment in vivo (Fig. 2C). Because of the complexity in the chromatographic resolution of **M4** and **M6**, their isobaric mass, as well as their identical MS/MS transitions, LC-MS/MS peak areas of these metabolites were grouped accordingly for the purpose of determining a semiquantitative plasma-time concentration profile and exposure analysis as a measure of the contribution of P450 in the metabolism of **1** in vivo. Although a decrease was observed in the C_{max} of **M4–M6** (0.64-fold), a 2.1-fold increase was observed in the AUC of these metabolites in the ABT-pretreated rats (Table 5). This observation may be due to alterations in the secondary metabolism and clearance mechanisms acting on **M4** and/or **M6**.

Discussion

Successful approaches have been developed to evaluate the impact of enzyme inhibitors and inducers on P450-mediated drug clearance and subsequent changes in drug exposure for prediction of clinical drug interactions (Zhang et al., 2009; Di et al., 2013); however, approaches toward predicting drug interaction potential of NCEs undergoing non-P450 metabolism are less well established, much less those exhibiting both P450 and AO clearance routes.

Recognition of AO and P450 contributions to the clearance of **1** in vitro and in vivo provided an opportunity to investigate how P450 inhibition may impact the disposition and PK of a mixed AO:P450 substrate and its metabolites. Similarities between rat and human in vitro metabolism of **1** permitted the use of rat as a nonclinical P450 inhibition model, which revealed a trend toward increased exposure to the AO metabolite **M1** in rats with ABT-attenuated P450 activity (Scheme 2). In principle, coadministration of a perpetrator drug could result in observed elevations in metabolite plasma levels as a consequence of several possible mechanisms: 1) decreased metabolite clearance due to inhibition of secondary metabolism, 2) metabolic activation (stimulation of enzyme activity), 3) enzyme induction, or 4) metabolic shunting toward the uninhibited pathway (e.g., AO) when another pathway is inhibited (e.g., P450). It is unlikely that the elevated **M1** levels were due to a decrease in **M1** clearance in rats pretreated with ABT, as the major **M1** clearance pathway in vitro was previously determined to be XO-mediated metabolism to **M2** (Morrison et al., 2012); and although the activation of AO has been previously suggested (Nirogi et al., 2014), the present increased **M1** formation observed in hepatic S9 fractions absent NADPH relative to NADPH-containing reactions indicate there is no contribution from an ABT-mediated cooperativity on AO. Furthermore, data from our laboratory outlining incubations of **1** with hepatocytes revealed no increase in **M1** formation when ABT was present (data not shown). Finally, although the induction of AOX1 in mice, rats, and rabbits (Garattini and Terao, 2012) has been demonstrated, an induction mechanism accounting for our observations is highly unlikely given the single dose study design and duration thereof. Our observed increase in **M1**, therefore, appears to have resulted primarily from a condition of increased substrate availability to AO when the P450 pathway(s) of metabolism was attenuated. In additional support of this mechanism, the decrease in NADPH-dependent S9 CL_{int} (P450 pathway), with a maintenance of NADPH-independent S9 CL_{int} (AO pathway) with increased concentrations of **1,** indicates a lower $K_{m,\ P450}$ relative to the $K_{m,\ AO}$, according to the relationship in eq. 2:

$$CL_{int,total} = \left(\frac{V_{max,AO}}{K_{m,AO} + S}\right) + \left(\frac{V_{max,P450}}{K_{m,P450} + S}\right)$$

where V_{max} is the enzyme's maximum reaction velocity, K_m is the substrate concentration that yields half the maximal velocity, and *S* is the substrate concentration. Incidentally, our findings associate an

TABLE 5

Pharmacokinetic (PK) parameters of metabolites M1, M2, and M4–M6 after i.p. administration of **1** (3 mg/kg) to control rats or rats pretreated with ABT

AUC and C_{max} of all metabolites reported as peak area ratio analyte/IS*h and analyte/IS, respectively. Data represent a mean (± S.D.). Statistical analysis performed using a two-tailed unpaired t test.

PK Parameter	M1			M2			M4–M6		
	Control (*n* = 3)	ABT (*n* = 4)	Mean Fold over Control	Control (*n* = 3)	ABT (*n* = 4)	Mean Fold over Control	Control (*n* = 3)	ABT (*n* = 4)	Mean Fold over Control
C_{max}	0.282 ± 0.223	2.07 ± 1.74	7.3	0.038 ± 0.028	0.419 ± 0.351	11	0.400 ± 0.389	0.255 ± 0.113	0.64
AUC_{0-inf}	0.432 ± 0.269	6.65 ± 6.41	15	0.109 ± 0.044	1.51 ± 1.36	14	0.280 ± 0.254	0.590 ± 0.160	2.1

TABLE 6

Systemic exposure of metabolites M1 and M2 after an i.p. administration of **1** (10 mg/kg) to control rats or rats pretreated with ABT, allopurinol, or allopurinol + ABT

Area under the curve reported as peak area ratio analyte/IS* h, as no authentic metabolite standards were available. Data represent a mean of n = 2 (± S.E.M). Statistical analyses performed using a two-tailed unpaired t test.

Metabolite	Control	ABT	Mean Fold over Control	Allopurinol	Mean Fold over Control	Allopurinol + ABT	Mean Fold over Control
M1	5.10 ± 3.79	46.3 ± 24.6	9.1	13.4 ± 3.98	2.6	74.9 ± 1.74**	15
M2	1.20 ± 1.10	17.1 ± 11.9	14	n/a	n/a	n/a	n/a

*$P < 0.05$; **$P < 0.01$.

increase in metabolite exposure with the coadministration of **1** and an enzyme inhibitor, whereas this type of DDI situation typically would be anticipated with coadministration of a victim drug and an enzyme inducer or stimulator. We might have expected this metabolic shunting observation to prevent an extensive increase in the AUC of **1**, with AO compensating for loss of P450 activity; however, as ABT is a *pan*-P450 inactivator, we have likely forced the shunt toward a single enzyme (AO), potentially limiting the capacity for compensation (vs. inhibiting one enzyme with the possibility of shunting toward multiple enzymes).

Whereas the **M4–M6** AUC unexpectedly increased in ABT-pretreated rats, the significant increase in AUC and decrease in the total body CL of parent **1** indicates that ABT did inhibit P450 metabolism of **1** in vivo. A possible explanation for this observation is that ABT also inhibited secondary metabolism of **M4–M6**. Alternatively, as **M4** and **M6** were quantified together, it is also possible that the AUC of one metabolite was increased, whereas that of the other was decreased, potentially resulting from differences in inhibitory activity toward enzymes responsible for formation and/or clearance of **M4** and **M6**. Prior studies of ABT inhibitory activity toward human P450 enzymes found that P450 2C9 is only minimally impacted by ABT (60% remaining activity after 30 minutes of pretreatment of human liver microsomes with 1 mM ABT) (Linder et al., 2009); the differential inhibitory activity of ABT toward rat P450 isoforms is unknown. Presently, we found an approximate 65% decrease in **M4** compared with a 25% increase in **M6** in pooled plasma samples (1–6 hours) from rats pretreated with ABT relative to control rats (Supplemental Fig. 3), indicating ABT may have differentially impacted the disposition of the two metabolites.

Besides significant increases in exposure to parent compound **1**, mean increases observed in the AUC and C_{max} of the AO metabolite **M1** highlight the potential for a drug interaction resulting from increased exposure to a metabolite of a drug with both AO and P450 clearance routes when coadministered with a P450 inhibitor. Clinically used drugs exhibiting a major clearance pathway via AO are few, and to date, no clinically relevant DDIs resulting from AO inhibition have been recognized, despite the identification of many clinical drugs demonstrating AO inhibition in vitro (Obach et al., 2004); however, our data indicate that inhibition of alternate clearance routes (e.g., P450) for drugs also metabolized by AO may result in elevation of a circulating AO-mediated metabolite, which, importantly, could have clinical implications when metabolites exhibit pharmacologic or toxicologic activity (Smith and Obach, 2005). For example, cases of dose-dependent renal toxicity associated with AO-mediated formation of a low-solubility metabolite have been reported for methotrexate (Smeland et al., 1996) and the two c-Met inhibitors SGX523 and JNJ-38877605, recently discontinued in clinical trials (Infante et al.,

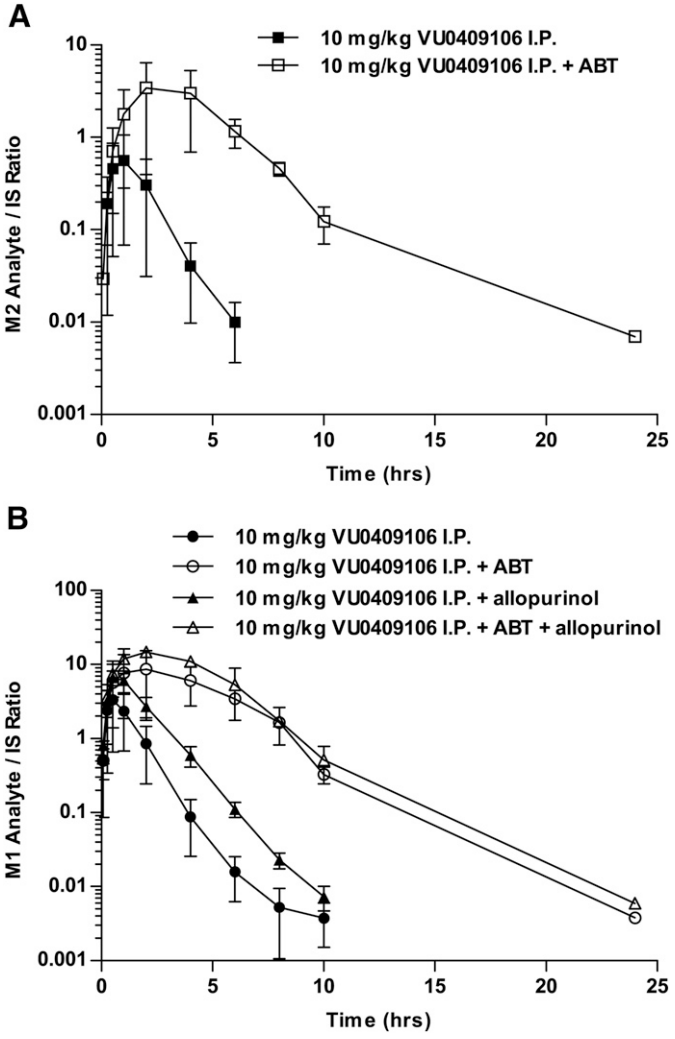

Fig. 3. Mean plasma concentration-time profiles of **M2** (A) or **M1** (B) after i.p. administration of VU0409106 (**1**) (10 mg/kg) to rats with or without an inhibitor. (A) Relative levels of **M2** in rats pretreated with ABT (open squares) versus vehicle (closed squares). (B) Relative levels of **M1** in rats pretreated with ABT (open circles), allopurinol (closed triangles), ABT + allopurinol (open triangles), or vehicle (closed circles). Data are expressed as the peak area ratio of analyte/internal standard and represent the mean (±S.E.M., $n = 2$).

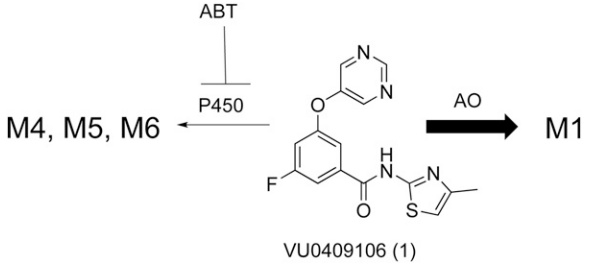

Scheme 2. Increase in **M1** formation observed in rats after ABT inhibition of P450.

2013; Lolkema et al., 2015). Additionally, the primary circulating metabolite of idealisib, GS-563117, is a mechanism-based inhibitor of P450 3A, which is not the case for the parent drug. In this instance, however, both AO and P450 3A (minor) contribute to the formation of GS-563117 (Ramanathan et al., 2016).

Although a small percentage of currently marketed drugs are cleared via AO, a recent study indicated that the proportion of NCEs in research and development containing potentially AO-susceptible moieties is much higher (Pryde et al., 2010). Drug-discovery scientists are more frequently encountering AO metabolism owing to incorporation of nitrogen-containing aromatic rings for either target engagement (e.g., kinases) or mitigation of P450 metabolism (reduced lipophilicity). As many AO substrates (e.g., zaleplon and idealisib) are known to also undergo metabolism via enzymes other than AO (Strelevitz et al., 2012; Ramanathan et al., 2016), it is likely that current and future NCEs exhibiting AO metabolism will also undergo metabolism via alternate enzymes. As such, metabolic shunting may be important to consider during toxicology and DDI assessment of these compounds. Likewise, this consideration may also be important for NCEs not displaying AO metabolism without concomitant administration of an enzyme inhibitor, yet containing an AO-susceptible structural moiety (potential for metabolic switching (Li et al., 2012a,b)). The likelihood of substantial elevations in metabolite exposure (via metabolic shunting) may be increased for drugs cleared by both AO and P450 enzymes versus drugs cleared only by multiple P450 pathways, as different P450 enzymes commonly generate the same metabolite, in which case the metabolite would be expected to be generated at decreased or similar levels when one of the P450 pathways is inhibited.

In conclusion, our studies with **1** and ABT using the rat as a nonclinical PK model revealed increased exposure to both the parent drug and the AO metabolite. The present investigation highlights the potential drug interactions that may occur with coadministration of a P450 inhibitor and a mixed AO/P450 substrate. The similarities we observed in vitro between SD rats and humans in the formation of AO and P450 metabolites, trends in the impact of P450 activity on the formation of **M1**, and in the kinetic behavior of the two enzymatic pathways indicate that our observations in vivo in rat may translate to human in vivo. We submit that the rat may offer a nonclinical model to probe drug interactions (and mechanisms thereof) where a mixed AO:P450 substrate experiences clinical drug interaction duress while underscoring the potential existence of the compound-dependent use of nonclinical models to predict AO-mediated interactions. As investigators are more frequently encountering AO metabolism through the drug discovery and development continuum, understanding the drug interaction potential for drugs exhibiting an AO clearance component will be important in the successful advancement and safe clinical implementation of future drug candidates bearing this non-P450 phenotype.

Acknowledgments

The authors thank Dr. J. Matthew Hutzler (Q2 Solutions) and Dr. W. Scott Akers (Lipscomb University College of Pharmacy) for helpful discussions regarding the present investigation.

Authorship Contributions

Participated in research design: Crouch, Morrison, Daniels.

Conducted experiments: Byers, Crouch, Morrison.

Contributed new reagents or analytical tools: Lindsley, Emmitte.

Performed data analysis: Crouch, Morrison, Daniels.

Wrote or contributed to the writing of the manuscript: Emmitte, Lindsley, Crouch, Daniels.

References

Al-Salmy HS (2001) Individual variation in hepatic aldehyde oxidase activity. *IUBMB Life* **51**: 249–253.

Barr JT and Jones JP (2011) Inhibition of human liver aldehyde oxidase: implications for potential drug-drug interactions. *Drug Metab Dispos* **39**:2381–2386.

Beedham C, Bruce SE, Critchley DJ, al-Tayib Y, and Rance DJ (1987) Species variation in hepatic aldehyde oxidase activity. *Eur J Drug Metab Pharmacokinet* **12**:307–310.

Beedham C, Critchley DJ, and Rance DJ (1995) Substrate specificity of human liver aldehyde oxidase toward substituted quinazolines and phthalazines: a comparison with hepatic enzyme from guinea pig, rabbit, and baboon. *Arch Biochem Biophys* **319**:481–490.

Coelho C, Foti A, Hartmann T, Santos-Silva T, Leimkühler S, and Romão MJ (2015) Structural insights into xenobiotic and inhibitor binding to human aldehyde oxidase. *Nat Chem Biol* **11**: 779–783.

Dalvie D, Sun H, Xiang C, Hu Q, Jiang Y, and Kang P (2012) Effect of structural variation on aldehyde oxidase-catalyzed oxidation of zoniporide. *Drug Metab Dispos* **40**:1575–1587.

Dalvie D, Xiang C, Kang P, and Zhou S (2013) Interspecies variation in the metabolism of zoniporide by aldehyde oxidase. *Xenobiotica* **43**:399–408.

Di L, Feng B, Goosen TC, Lai Y, Steyn SJ, Varma MV, and Obach RS (2013) A perspective on the prediction of drug pharmacokinetics and disposition in drug research and development. *Drug Metab Dispos* **41**:1975–1993.

Diamond S, Boer J, Maduskuie TP, Jr, Falahatpisheh N, Li Y, and Yeleswaram S (2010) Species-specific metabolism of SGX523 by aldehyde oxidase and the toxicological implications. *Drug Metab Dispos* **38**:1277–1285.

Garattini E and Terao M (2012) The role of aldehyde oxidase in drug metabolism. *Expert Opin Drug Metab Toxicol* **8**:487–503.

Hartmann T, Terao M, Garattini E, Teutloff C, Alfaro JF, Jones JP, and Leimkühler S (2012) The impact of single nucleotide polymorphisms on human aldehyde oxidase. *Drug Metab Dispos* **40**:856–864.

Hutzler JM, Yang Y-S, Brown C, Heyward S, and Moeller T (2014) Aldehyde oxidase activity in donor-matched fresh and cryopreserved human hepatocytes and assessment of variability in 75 donors. *Drug Metab Dispos* **42**:1090–1097.

Infante JR, Rugg T, Gordon M, Rooney I, Rosen L, Zeh K, Liu R, Burris HA, and Ramanathan RK (2013) Unexpected renal toxicity associated with SGX523, a small molecule inhibitor of MET. *Invest New Drugs* **31**:363–369.

Kitamura S, Sugihara K, Nakatani K, Ohta S, Ohhara T, Ninomiya S, Green CE, and Tyson CA (1999) Variation of hepatic methotrexate 7-hydroxylase activity in animals and humans. *IUBMB Life* **48**:607–611.

Li Y, Lai WG, Whitcher-Johnstone A, Busacca CA, Eriksson MC, Lorenz JC, and Tweedie DJ (2012a) Metabolic switching of BILR 355 in the presence of ritonavir. I. Identifying an unexpected disproportionate human metabolite. *Drug Metab Dispos* **40**:1122–1129.

Li Y, Xu J, Lai WG, Whitcher-Johnstone A, and Tweedie DJ (2012b) Metabolic switching of BILR 355 in the presence of ritonavir. II. Uncovering novel contributions by gut bacteria and aldehyde oxidase. *Drug Metab Dispos* **40**:1130–1137.

Linder CD, Renaud NA, and Hutzler JM (2009) Is 1-aminobenzotriazole an appropriate in vitro tool as a nonspecific cytochrome P450 inactivator? *Drug Metab Dispos* **37**:10–13.

Lolkema MP, Bohets HH, Arkenau HT, Lampo A, Barale E, de Jonge MJ, van Doorn L, Hellemans P, de Bono JS, and Eskens FA (2015) The c-met tyrosine kinase inhibitor JNJ-38877605 causes renal toxicity through species-specific insoluble metabolite formation. *Clin Cancer Res* **21**:2297–2304.

Morrison RD, Blobaum AL, Byers FW, Santomango TS, Bridges TM, Stec D, Brewer KA, Sanchez-Ponce R, Corlew MM, and Rush R, et al. (2012) The role of aldehyde oxidase and xanthine oxidase in the biotransformation of a novel negative allosteric modulator of metabotropic glutamate receptor subtype 5. *Drug Metab Dispos* **40**:1834–1845.

Nirogi R, Kandikere V, Palacharla RC, Bhyrapuneni G, Kanamarlapudi VB, Ponnamaneni RK, and Manoharan AK (2014) Identification of a suitable and selective inhibitor towards aldehyde oxidase catalyzed reactions. *Xenobiotica* **44**:197–204.

Obach RS, Huynh P, Allen MC, and Beedham C (2004) Human liver aldehyde oxidase: inhibition by 239 drugs. *J Clin Pharmacol* **44**:7–19.

Prueksaritanont T, Chu X, Gibson C, Cui D, Yee KL, Ballard J, Cabalu T, and Hochman J (2013) Drug-drug interaction studies: regulatory guidance and an industry perspective. *AAPS J* **15**: 629–645.

Prueksaritanont T, Kuo Y, Tang C, Li C, Qiu Y, Lu B, Strong-Basalyga K, Richards K, Carr B, and Lin JH (2006) In vitro and in vivo CYP3A64 induction and inhibition studies in rhesus monkeys: a preclinical approach for CYP3A-mediated drug interaction studies. *Drug Metab Dispos* **34**:1546–1555.

Pryde DC, Dalvie D, Hu Q, Jones P, Obach RS, and Tran T-D (2010) Aldehyde oxidase: an enzyme of emerging importance in drug discovery. *J Med Chem* **53**:8441–8460.

Ramanathan S, Jin F, Sharma S, and Kearney BP (2016) Clinical pharmacokinetic and pharmacodynamic profile of idelalisib. *Clin Pharmacokinet* **55**:33–45.

Sahi J, Khan KK, and Black CB (2008) Aldehyde oxidase activity and inhibition in hepatocytes and cytosolic fractions from mouse, rat, monkey and human. *Drug Metab Lett* **2**: 176–183.

Smeland E, Fuskevåg OM, Nymann K, Svendesn JS, Olsen R, Lindal S, Bremnes RM, and Aarbakke J (1996) High-dose 7-hydromethotrexate: acute toxicity and lethality in a rat model. *Cancer Chemother Pharmacol* **37**:415–422.

Smith DA and Obach RS (2005) Seeing through the mist: abundance versus percentage. Commentary on metabolites in safety testing. *Drug Metab Dispos* **33**:1409–1417.

Strelevitz TJ, Orozco CC, and Obach RS (2012) Hydralazine as a selective probe inactivator of aldehyde oxidase in human hepatocytes: estimation of the contribution of aldehyde oxidase to metabolic clearance. *Drug Metab Dispos* **40**:1441–1448.

Zhang L, Zhang YD, Zhao P, and Huang SM (2009) Predicting drug-drug interactions: an FDA perspective. *AAPS J* **11**:300–306.

Address correspondence to: Dr. J. Scott Daniels, Sano Informed Prescribing, Inc. 393 Nichol Mill Ln, Franklin, TN 37067. E-mail: scott@thinksano.com

Evaluating the Disposition of a Mixed Aldehyde Oxidase/Cytochrome P450 Substrate in Rats with Attenuated P450 Activity

Rachel D. Crouch, Ryan D. Morrison, Frank W. Byers, Craig W. Lindsley, Kyle A. Emmitte and J. Scott Daniels

Supplemental Information.

Supplemental Figure 1.

LC/MS^3 of Metabolite, M6, detected in SD rat and human hepatic microsomes. A subsequent full scan LC/MS experiment (see inset) where the mobile phase A buffer (10 mM NH_4^+ formate) was prepared in D_2O (deuterium exchange experiment) produced an $[M+D]^+$ for **M6** at *m/z* 350 Da, indicative of a hydroxylation of a carbon atom of the thiazole moiety; versus that of an *N*- or *S*-oxidation (calculated, $[M+D]^+$ of 349 Da).

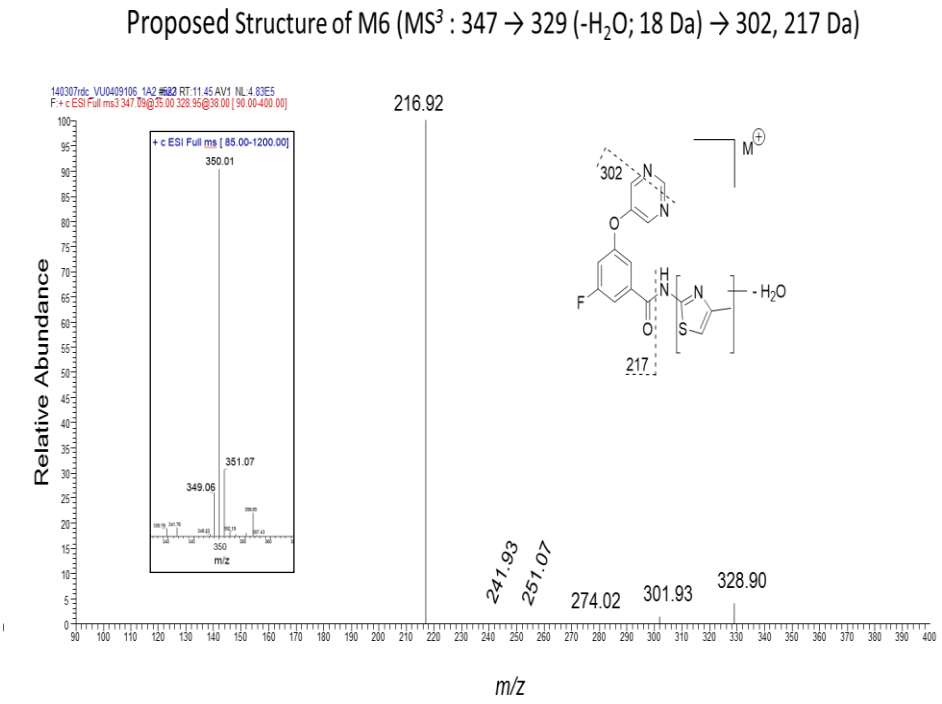

Supplemental Figure 2.

Representative mean plasma concentration-time profiles from SD rats receiving **(A)** 50 mg/kg ABT P.O. followed by 3 mg/kg of **1** I.P. or **(B)** 50 mg/kg allopurinol P.O. followed by 10 mg/kg of **1** I.P. Each data point represents the mean ± SD, n = 4 **(A)** or ±SEM, n = 2 **(B)**. ABT or allopurinol was administered 2 hours prior to t = 0, which represents the time at which **1** was administered. Some data points were above the upper limit of quantitation (10,000 ng/mL), and thus, these data points represent concentrations that are ≥ 10,000 ng/mL.

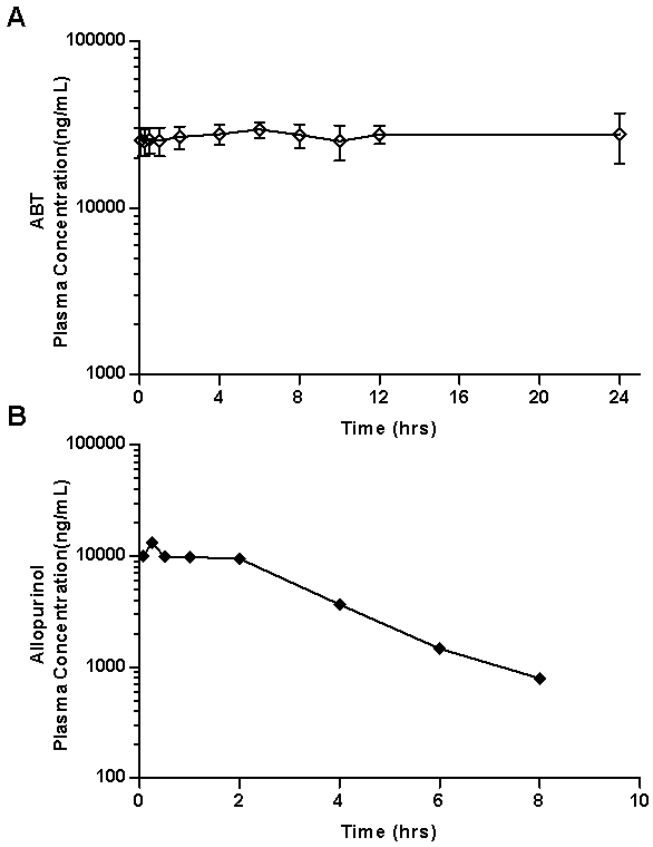

Supplemental Figure 3.

LC/MS chromatograms representing total ion current (TIC) of ms^2 347 detected in extracts of pooled plasma collected between 1-6 hours from rats receiving 10 mg/kg of **1** alone (A) or pretreated with 50 mg/kg ABT (B).